Experimental-based mechanobiological modeling of the anabolic and catabolic effects of breast cancer on bone remodeling

Imane Ait Oumghar, Abdelwahed Barkaoui, Patrick Chabrand, Abdellatif El Ghazi, Charlotte Jeanneau, Daphne Guenoun, Peter Pivonka

Experimental-based mechanobiological modeling of the anabolic and catabolic effects of breast cancer on bone remodeling

Imane Ait Oumghar[1,2] · Abdelwahed Barkaoui[1] · Patrick Chabrand[2] · Abdellatif El Ghazi[3] · Charlotte Jeanneau[2] · Daphne Guenoun[2] · Peter Pivonka[4]

Abstract
Bone is a biological tissue characterized by its hierarchical organization. This material has the ability to be continually renewed, which makes it highly adaptative to external loadings. Bone renewing is managed by a dynamic biological process called bone remodeling (BR), where continuous resorption of old bone and formation of new bone permits to change the bone composition and microstructure. Unfortunately, because of several factors, such as age, hormonal imbalance, and a variety of pathologies including cancer metastases, this process can be disturbed leading to various bone diseases. In this study, we have investigated the effect of breast cancer (BC) metastases causing osteolytic bone loss. BC has the ability to affect bone quantity in different ways in each of its primary and secondary stages. Based on a BR mathematical model, we modeled the BC cells' interaction with bone cells to assess their effect on bone volume fraction (BV/TV) evolution during the remodeling process. Some of the parameters used in our model have been determined experimentally using the enzyme-linked immune-sorbent assay (ELISA) and the MTT assay. Our numerical simulations show that primary BC plays a significant role in enhancing bone-forming cells' activity leading to a 6.22% increase in BV/TV over 1 year. On the other hand, secondary BC causes a noticeable decrease in BV/TV reaching 15.74% over 2 years.

Keywords Bone · Bone remodeling · Breast cancer · Bone volume fraction · Mathematical modeling

1 Introduction

Breast cancer is the most common disease affecting women worldwide. According to (Labrie 2015), 1,1 billion women are susceptible to be affected by 2025. Nowadays, 60% of cases are diagnosed as hormonal dependent, usually sensitive to estrogen (E) and progesterone (PR) hormones (Lumachi 2015). After migration, BC tumor cells affect directly the bone cells by secreting different types of cytokines. Those interactions most often lead to osteolytic morbidity or also osteoblastic and mixed morbidities (Kozlow and Guise 2005). Apart from the direct effect of breast cancer on bone cells occurring when BC metastasizes to bone, primary tumor cells can also affect bone through circulation of their secreted substances inducing perturbed bone growth (Chiou et al. 2021).

Bone tissue deterioration because of BC is tightly related to the disruption of bone metabolism. BR, as a controlling mechanism, is a biochemical process monitored by many biological and mechanical factors. In order to maintain bone strength, the BR mechanism allows the renewal of bone matrix through the balance of resorption and formation phases. Osteoclasts and osteoblasts are the main bone cells interacting in the so-called basic multicellular units (BMU) during this process. After the activation of mechanosensory bone cells called osteocytes, which are located in the bone matrix, the osteoclasts resorbing the bone, are activated. Thereafter, osteoblasts arrive into the created bone gap and start to form the new bone matrix. There are many biological factors controlling bone cells' behavior during

✉ Abdelwahed Barkaoui
abdelwahed.barkaoui@uir.ac.ma

1 LERMA Lab, Université Internationale de Rabat, Rocade Rabat Salé 11100, Rabat-Sala El Jadida, Morocco

2 Université Aix-Marseille, ISM, 163 av. de Luminy, 13288 Marseille Cedex 09, France

3 TIC Lab, Université Internationale de Rabat, Rocade Rabat Salé 11100, Rabat-Sala El Jadida, Morocco

4 Biomechanics and Spine Research Group, Queensland University of Technology at the Centre for Children's Health Research, South Brisbane 4101, QLD, Australia

the process. RANKL/RANK/OPG pathway, which was discovered in the mid-90s, is a major signaling pathway that was enormously investigated by researchers to understand and explain the bone cell and cell–cell interactions. It consists of three essential molecules: (i) the receptor activator of nuclear factor (NF)-κB (RANK) expressed by osteoclasts, (ii) the receptor activator of nuclear factor (NF)-κB Ligand (RANKL), and (iii) osteoprotegerin (OPG) released by osteoblasts. This system controls osteoclasts' differentiation and activation during BR. RANK–RANKL binding stimulates the osteoclastogenesis, while OPG–RANKL binding protects the bone from excessive resorption by preventing RANK–RANKL binding.

Several mathematical models had been proposed and developed in order to study bone cells' behavior and explain the experimental observations related to bone biology during the remodeling cycle. Most of them are based on (Frost 1969; Mullender and Huiskes 1997) theories, which, respectively, study the bone mass variation based on local deformation and deformation energy density during the process. In 2003, the first dynamic model considering bone cells behavior has been proposed by Komarova et al. (2003), where autocrine and paracrine interactions among osteoclasts and osteoblasts are included. Based on this work, and others, (Lemaire et al. 2004) constructed another dynamic model incorporating RANKL/RANK/OPG biochemical pathway effect in addition to other biochemical factors controlling the BR process. In 2008, Lemaire's model has been further developed by Pivonka et al. (2008), then analyzed to find out an accurate model structure based on RANKL and OPG's expression on osteoblasts at different stages of maturation.

The mathematical models of BR have been used in several studies to represent the pathophysiological mechanism within a diseased bone. Each of osteoporosis, Paget's disease of bone, cancer-related bone degradation such as multiple myeloma and prostate cancer have been investigated in the literature using BR mathematical models (Ait Oumghar et al. 2020; Oumghar et al. 2021). Nevertheless, breast cancer effect on BR has not been studied in detail.

In the present work, we seek to study the effect of breast cancer on the variation of bone volume fraction (BV/TV) via a mathematical modeling of the BR disturbance at the primary and metastatic stages of breast cancer. Model parameters for breast cancer were determined experimentally by enzyme-linked immunosorbent (ELISA) and MTT assays. The primary BC has been represented by the effect of extracellular vesicles (EV) released by tumor on RANKL, interlukeine-6 (IL-6), and OPG secretion by osteoblasts. For the secondary BC, it has been represented by including their secretion of parathyroid hormone-related peptide (PTHrP), IL-6, dickkopf-1 (DKK-1), wingless-related integration site (Wnt), and RANKL effect on RANKL/RANK/OPG pathway perturbation. Additionally to BC effect, estrogen's level influence on the BR process has been considered to reflect the menopausal state.

The steps followed in this study are:(i) a thorough literature study to identify the relationship between breast cancer and osteoporosis (explanatory figures have been elaborated), (ii) proposed a mathematical model of bone remodeling with the effect of primary cancer, (iii) mathematically model the effect of secondary breast cancer, and (iv) carry out experimental trials to determine the model parameters in relation to breast cancer.

2 Breast cancer/bone biology

After menopause, ovaries cease to produce estrogen. But concurrently, the hypothalamus continues to release the gonadotropin-releasing hormone (GnRH) entering in E stimulation through dehydroepiandrosterone (DHEA) and dehydroepiandrosterone sulfate (DHEA-S) actions (Labrie 2015) (Fig. 1). DHEA activates of aromatase conversion of androgen into estrogen (De Mukhopadhyay et al. 2015) and DHEA-S is converted to estradiol by means of breast tissue secreted enzymes such as 3β-HSD and 17β-HSD1 (Bhardwaj et al. 2019). Breast tissue is mainly composed of two epithelial cell types: (i) the luminal epithelial cells (LECs) and (ii) the basal myoepithelial cells (MECs) (Kiesel and Kohl 2016). These cells express various receptors including estrogen receptors (ER), progesterone receptor (PR), and RANK.

In our model tumor cells proliferation would be controlled by only E in primary BC state and by E, RANKL, Wnt, IL-6, and TGFβ available in bone microenvironment in secondary BC state.

According to (Mundy 2002), bidirectional interactions are created between BC metastatic cells and bone cells in the bone microenvironment creating a vicious cycle leading to osteolytic lesions and tumor growth. BC tumor cells secrete various cytokines such as RANKL, parathyroid hormone (PTH) and the group of interleukins IL-1, IL-6, IL-8, macrophage colony-stimulating factor (M-CSF), DKK-1, prostaglandin E2 (PGE2), and PTHrP (Clézardin 2011). Those cytokines inhibit bone formation and stimulate bone resorption (Fig. 2). Besides, BC tumor cells RANK expression makes the bone microenvironment favorable for their proliferation (Blake et al. 2014). During bone resorption, some bone growth factors are released in the bone microenvironment such as vascular endothelial growth factor (VEGF), insulin-like growth factor (IGF), fibroblast growth factor (FBFs), and the transforming growth factor β (TGFβ) (Salamanna et al. 2018). All those substances are promoting epithelial tumor cell proliferation of which TGFβ stimulate additionally the PTHrP expression by tumor cells.

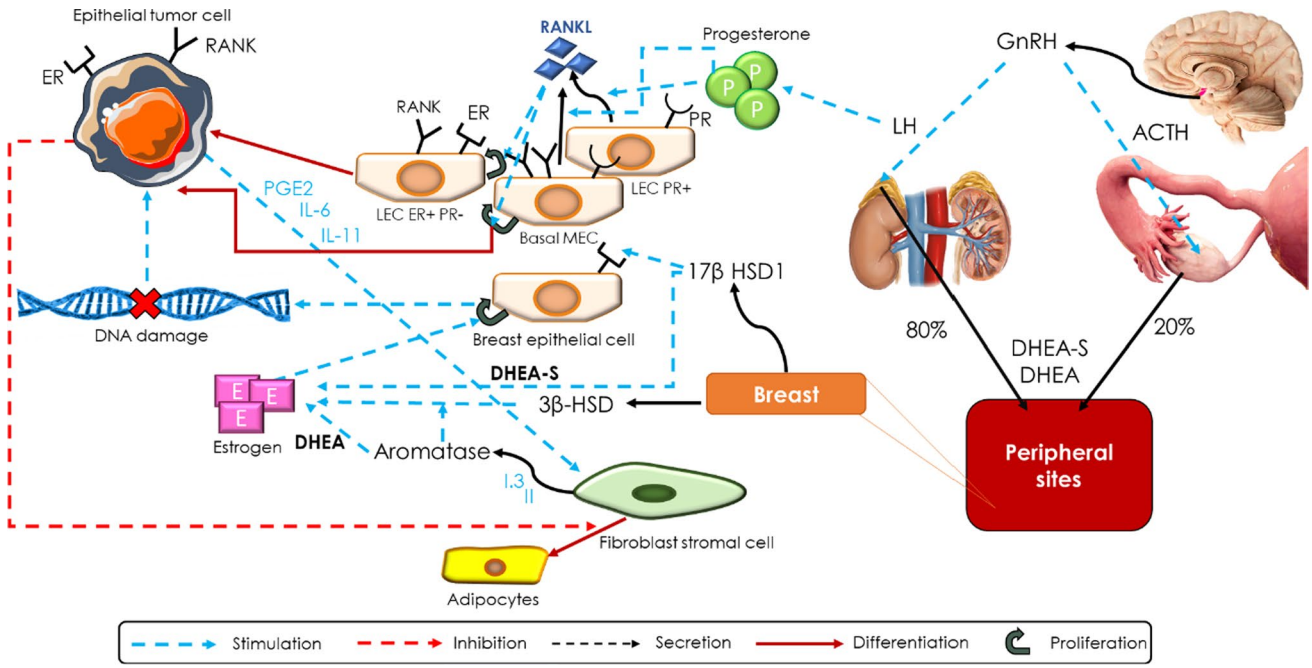

Fig. 1 Schematic representation of breast cancer cell formation, growth, and proliferation under estrogen and progesterone actions in postmenopausal women. GnRH stimulates DHEA and DHEA-S secretion by ovaries and adrenal glands through the action of ACTH synthesis. DHEA and DHEA-S mediate E production by peripheral sites including the breast. LEC cells expressing ER proliferate due to increased E leading to DNA damage. Besides E, PR production by adrenal gland increases under LH effect and stimulates LEC PR + cells' proliferation and their secretion of RANKL. RANKL induces the proliferation of LEC ER + and PR-cells and MEC cells expressing RANK. Tumor cells created because of excessive proliferation inhibit their differentiation into adipocytes leading to increased E. (Developed by the authors)

3 Material and methods

3.1 Formulation of a mechanistic bone cell–BC cell interaction model

Based on the understanding of the link between BC and bone presented in the previous section (Figs. 1 and 2), we developed a mathematical model which extends the bone cell population model of (Pivonka et al. 2008; Scheiner et al. 2013) toward BR–BC cell interactions, by incorporating estrogen and BC secreted factors into the biochemical pathways of the BR process. In this work, the normal BR model of Pivonka et al. (2008; Scheiner et al. 2013) has been simulated using (Wang et al. 2011) parameters and DKK-1, Wnt, and IL-6 effect in normal conditions have been added before calibration (see Appendix). Based on this model, we added primary BC effect through the extracellular vesicles (EV) particles effect on IL-6, RANKL, and OPG concentrations; and secondary BC effect through their secreted factors in the bone microenvironment (Fig. 3).

3.1.1 Modeling primary BC–BR model

In its premetastatic stage, breast cancer is capable to affect the bone microenvironment. According to (Chiou et al. 2021), tumor-derived factors induce an abnormal mineralized bone. Based on their experiments, authors have detected an increase in bone thickness and BV/TV in both cortical and trabecular bone. This enhancement of bone formation has been justified by the action of tumor signals action on osteoblasts behavior. For the BC case, the EV target the bone microenvironment and could be taken up by bone cells causing the observed alteration in bone architecture and quality (Chiou et al. 2021).

To mimic the EV effect on bone cells behavior, we have considered the results of (Loftus et al. 2019), which provided the effect of EV secreted by ER + breast cancer cells MCF-7 on osteoblasts. Accordingly, eightfold increase, twofold increase, and fourfold decrease in RANKL, IL-6, and OPG production by osteoblasts have been detected, respectively. To model those interactions, we have made modifications upon the normal BR model (Table 1).

Each of $F_{\mathrm{EV,RANKL}}$, $F_{\mathrm{EV,OPG}}$, and $F_{\mathrm{EV,IL6}}$ depends on BC cells' concentration in the breast environment $C_{T'}$. In the following equation, we represent the differential equation of tumor cells concentration evolution over time:

$$\frac{dC_{T'}(t)}{dt} = P_{T'}\pi^{T'}_{\mathrm{act},E} ln\left(\frac{C_{T'\max}}{C_{T'}}\right)C_{T'} \quad (1)$$

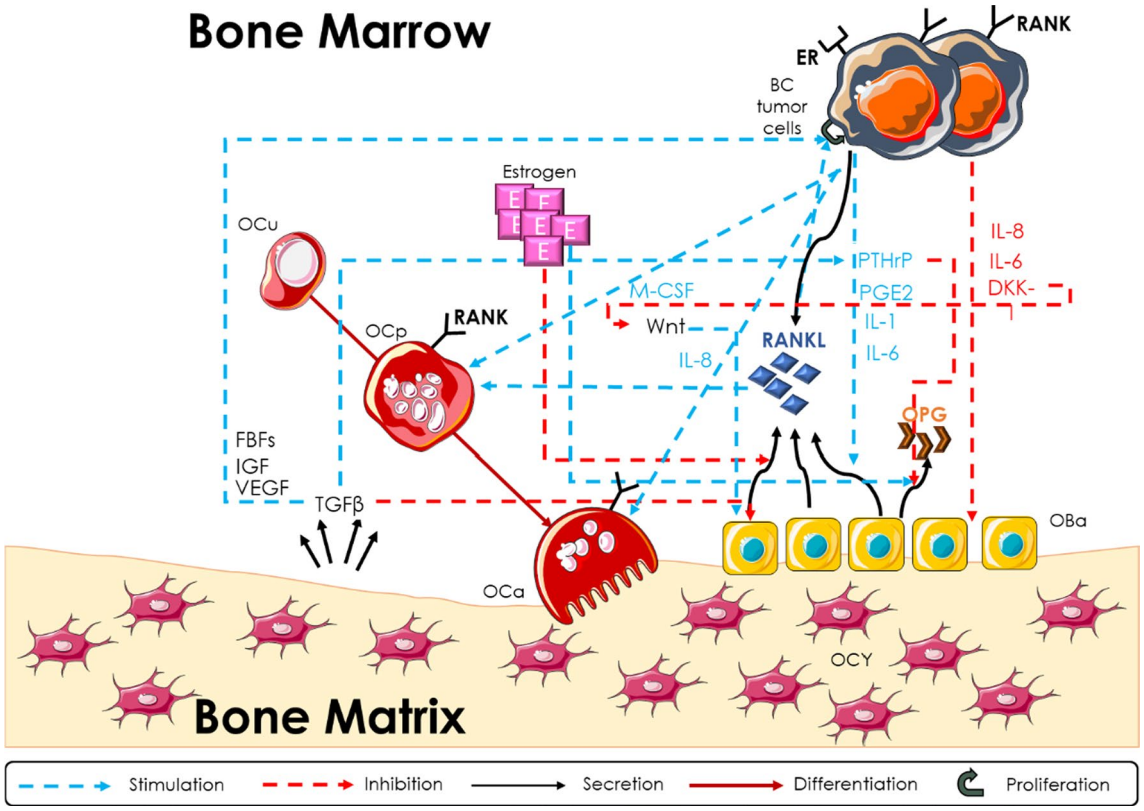

Fig. 2 Schematic representation of breast cancer (BC) tumor cells interactions with bone cells in the bone microenvironment during BR process in postmenopausal women. BC cells. (Developed by the authors)

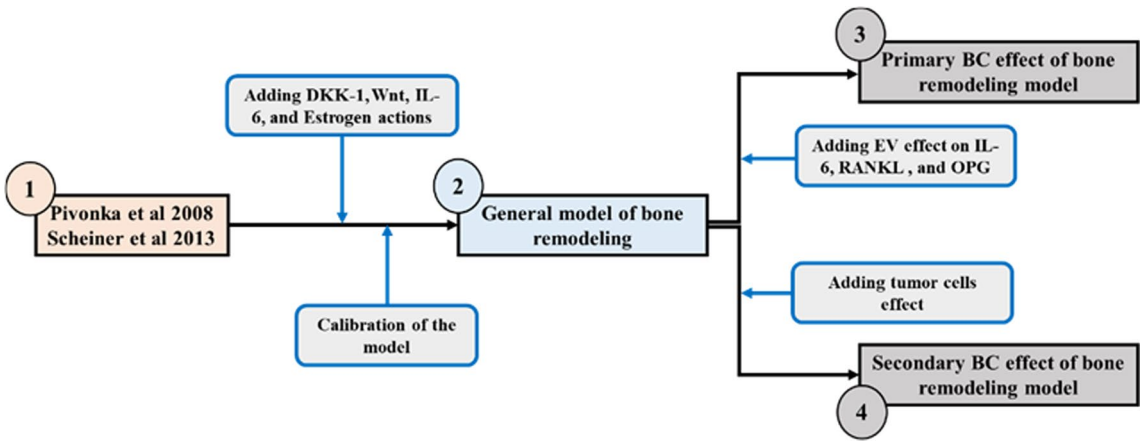

Fig. 3 Modification steps of the bone remodeling process to incorporate the effect of primary and secondary BC cells

The activation function of tumor proliferation $\pi_{\mathrm{act},E}^{T'}$ is the Hill action function of E, $P_{T'}$ is the proliferation rate of primary BC cells, and $C_{T'\max}$ is the carrying capacity of primary BC cells concentration.

3.1.2 Modeling secondary BC–BR model

In Fig. 4, the BC–bone cells interaction considered in the formulation of our mathematical model is presented. The main biochemical factor incorporated in the model is: the RANK/RANK/OPG pathway regulating osteoclasts' differentiation; Wnt and DKK-1 regulating osteoblasts

Table 1 Description of the biochemical factors' integration modification in the BR model under primary BC

Original function	Modified function
$C_{\mathrm{RANKLmax}} = R_{\mathrm{RL,OBp}} C_{\mathrm{OBp}} \pi_{\mathrm{RANKL}}^{\mathrm{Ligand}}$	$C_{\mathrm{RANKLmax}} = R_{\mathrm{RL,OBp}} C_{\mathrm{OBp}} \pi_{\mathrm{RANKL}}^{\mathrm{Ligand}} \boldsymbol{F_{EV,RANKL}}$
	$\boldsymbol{F_{EV,RANKL}} = L_{\mathrm{EV,RANKL}} C_{T'}$
$C_{\mathrm{OPG}} = \frac{(\beta_{\mathrm{OBa,OPG}} C_{\mathrm{OBa}}) \pi_{\mathrm{OPG}}^{\mathrm{Ligand}}}{\frac{(\beta_{\mathrm{OBa,OPG}} C_{\mathrm{OBa}}) \pi_{\mathrm{rep,OPG}}^{\mathrm{Ligand}}}{C_{\mathrm{OPGmax}}} + \widetilde{D_{\mathrm{OPG}}}}$	$C_{OPG} = \frac{(\beta_{OBa,\mathrm{OPG}} C_{OBa}) \pi_{OPG}^{Ligand} \boldsymbol{F_{EV,OPG}}}{\frac{(\beta_{OBa,\mathrm{OPG}} C_{OBa}) \pi_{rep,OPG}^{Ligand} \boldsymbol{F_{EV,OPG}}}{C_{OPGmax}} + \widetilde{D_{OPG}}}$
	$F_{\mathrm{EV,OPG}} = L_{\mathrm{EV,OPG}} / C_{T'}$
$C_{IL6} = \frac{(\beta_{IL6} C_{\mathrm{OBa}}) \pi_{\mathrm{act,TGF}}^{IL6}}{\frac{(\beta_{IL6} C_{\mathrm{OBa}}) \pi_{\mathrm{act,TGF}}^{IL6}}{C_{IL6max}} + \widetilde{D_{IL6}}}$	$C_{\mathrm{IL6}} = \frac{(\beta_{\mathrm{IL6}} C_{\mathrm{OBa}}) \pi_{\mathrm{act,TGF}}^{\mathrm{IL6}} \boldsymbol{F_{EV,IL6}}}{\frac{(\beta_{\mathrm{IL6}} C_{\mathrm{OBa}}) \pi_{\mathrm{act,TGF}}^{\mathrm{IL6}} \boldsymbol{F_{EV,IL6}}}{C_{\mathrm{IL6max}}} + \widetilde{D_{\mathrm{IL6}}}}$
	$\boldsymbol{F_{EV,IL6}} = L_{EV,IL6} C_{T'}$
C_E = constant	$C_E = 8.151 \times 10^1 pM$ (postmenopausal women)

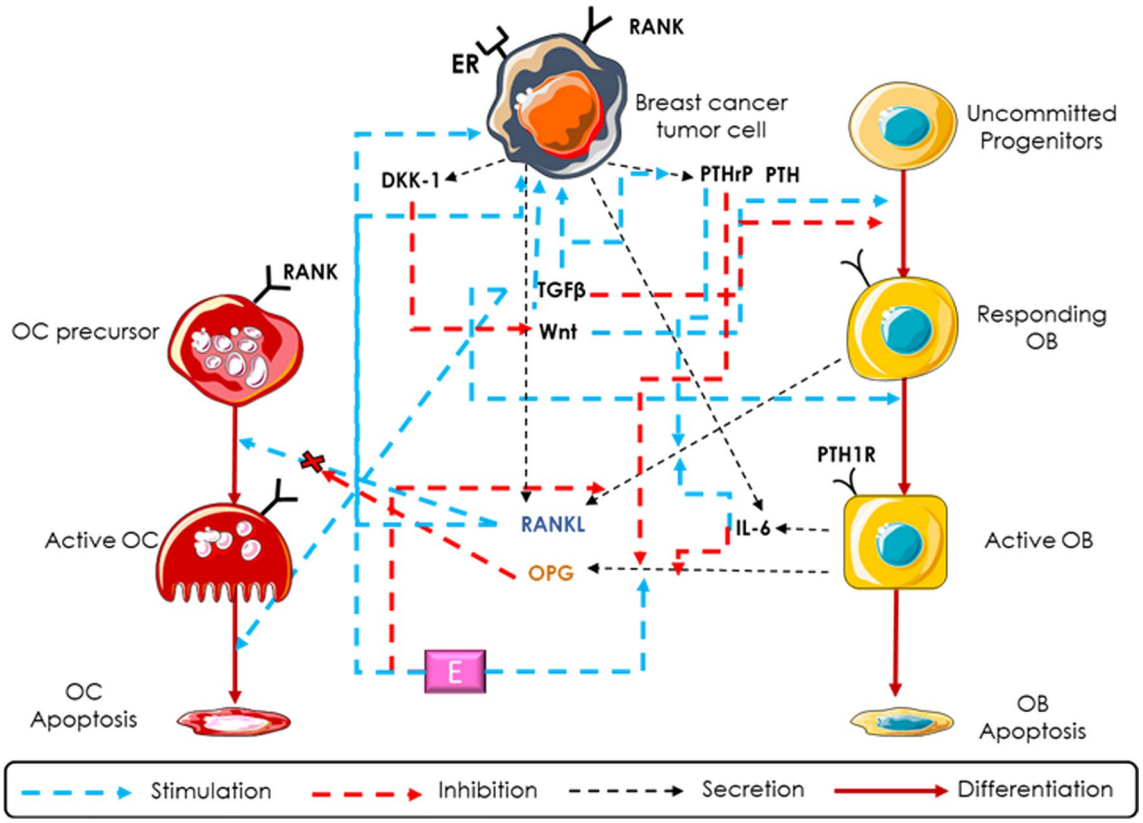

Fig. 4 Schematic representation of secondary breast cancer tumor cells interactions with bone cells during BR process (Developed by the authors)

differentiation, TGF_{β} regulating osteoblasts' differentiation, osteoclasts apoptosis, and tumor cells proliferation; and PTH, PTHrP, IL-6, and estrogen regulating RANKL and OPG's concentrations.

Wnt and DKK-1 concentrations increases in women with breast cancer (Lamb et al. 2013; Kasoha et al. 2018), where DKK-1 inhibits Wnt production by tumor cells. DKK-1 is only secreted by BC cells after metastasis based on our ELISA experimentations (Table 2).

PTHrP, IL-6, and E levels influence preosteoclasts' differentiation through the activation function of RANK–RANKL binding. Both the OPG concentration C_{OPG} and the maximum concentration of RANKL C_{RANKLmax} are regulated by PTH, PTHrP, IL-6, and E. PTH, PTHrP, and IL-6 repressing OPG production and stimulating the RANKL one, while E stimulating OPG production and repressing the RANKL one (Table 3).

In this model, each of DKK-1, Wnt, PTHrP, and IL-6 are synthetized by BC tumor cells. BC cells' concentration in the bone microenvironment C_T is determined by Eq. 2.

$$\frac{dC_T(t)}{dt} = X_T C_{T'\max} + P_T \pi_{\text{act}}^T \ln\left(\frac{C_{T\max}}{C_T}\right) C_T \tag{2}$$

X_T is the migration rate of primary BC cells, P_T is the proliferation rate of metastatic BC cells, and $C_{T\max}$ is the carrying capacity of secondary BC cells concentration. In this work, we presume that the proliferation action starts after a migration of a specific amount of primary BC cells (Del Monte 2009), and we consider two scenarios: (i) BC primary cells keep migrating after reaching their maximum amount in the breast and $X_T \neq 0$ (ii) BC primary cells stop migrating into the bone and only proliferation is considered $X_T = 0$.

Table 2 The results of the ELISA and MTT assay

Parameter	Value	Unit	Assay
$\widetilde{D_{\text{DKK1}}}$	1.525×10^{-1}	1/day	ELISA
$\beta_{\text{OBa,DKK1}}$	1.18×10^{5}	1/day	ELISA
$\beta_{\text{OBa,IL6}}$	2.085×10^{4}	1/day	ELISA
$\beta_{\text{OBp,RANKL}}$	1.6242×10^{2}	pM/day	ELISA
$\beta_{\text{T,RANKL}}$	3.83×10^{-8}	pM/day	ELISA
$\beta_{\text{OBp,DKK1}}$	0	1/day	ELISA
$\beta_{T,\text{DKK1}}$	1.09×10^{5}	1/day	ELISA
$\beta_{\text{OBa,IL6}}$	3.16×10^{4}	1/day	ELISA
$\beta_{T,\text{IL6}}$	8.4×10^{3}	1/day	ELISA
$R_{\text{RL},T}$	4.06×10^{4}	pM	ELISA
$\rho_{T,\text{RANK}}$	1.07×10^{-4}	pM	ELISA
$P_{T'}$	2.57×10^{-1}	1/day	MTT

The activation function of tumor proliferation π_{act}^T depends on the Hill action function assembling the effect of TGF_β, Wnt, RANK–RANKL, and E (Eq. 3). No synergic interaction is supposed between these cytokines.

$$\begin{aligned}\pi_{\text{act}}^T = [&\left(\pi_{\text{act,TGF}}^T + \pi_{\text{act,Wnt}}^T + \pi_{\text{act,IL6}}^T + \pi_{\text{act},E}^T + \pi_{\text{act,[RANK.RANKL]}}^T\right]\\ &- \left[\left(\pi_{\text{act,TGF}}^T \pi_{\text{act,Wnt}}^T\right) + \left(\pi_{\text{act,TGF}}^T \pi_{\text{act,IL6}}^T\right) + \left(\pi_{\text{act,TGF}}^T \pi_{\text{act},E}^T\right)\right.\\ &+ \left(\pi_{\text{act,TGF}}^T \pi_{act,\text{[RANK.RANKL]}}^T\right) + \left(\pi_{\text{act,Wnt}}^T \pi_{\text{act,IL6}}^T\right) + \left(\pi_{\text{act,Wnt}}^T \pi_{\text{act},E}^T\right)\\ &+ \left(\pi_{\text{act,Wnt}}^T \pi_{\text{act,[RANK.RANKL]}}^T\right) + \left(\pi_{\text{act,IL6}}^T \pi_{\text{act},E}^T\right)\\ &+ \left(\pi_{\text{act,IL6}}^T \pi_{\text{act,[RANK.RANKL]}}^T\right) + \left(\pi_{\text{act},E}^T \pi_{\text{act,[RANK.RANKL]}}^T\right).\end{aligned} \tag{3}$$

3.2 Algorithmic model formulation

The present model has been implemented by taking into consideration two driving inputs: (i) the BC models, and (ii) the mechanical loadings. The BC permitted to impact bone cells behavior through EV's action or by their biochemical secretions that impact the RANK/RANKL/OPG pathway, while the mechanical stimuli affected bone cells through the $\Pi_{\text{act,OBp}}^{\text{mech}}$ and $P_{\text{RANKL}}^{\text{mech}}$ functions. Resulted BV/TV controlled by bone cells closes the mechanical feedback loop (Fig. 5). The model differential equations have been resolved on a diurnal timescale over 1 year for normal conditions, 3 years for menopause, 1 year for primary BC, and 2 years for secondary BC. The integrity of our model equations has been programmed on MATLAB software and all the dynamic behaviors of drugs and cells have been calculated using numerical integration by the fourth-order Runge–Kutta method.

Table 3 Description of biochemical factors incorporation in the BR model under metastatic breast cancer

Original function	Modified function
$C_{\text{Wnt}} = \frac{\beta_{\text{Wnt}}.\pi_{\text{rep,DKK1}}}{\widetilde{D_{\text{Wnt}}}}$	$C_{\text{Wnt}} = \frac{(\beta_{\text{Wnt}}+\beta_{\text{Wnt},T}C_T)\pi_{\text{rep,DKK1}}}{\widetilde{D_{\text{Wnt}}}}$
	$\beta_{\text{Wnt,T}} = \beta_{\text{Wnt},T}^{\max}\frac{e^{(t-t_{\text{Wnt}})/\tau_{\text{Wnt}}}+\beta_{\text{Wnt},T}^{\min}/\beta_{\text{Wnt},T}^{\max}}{e^{(t-t_{\text{Wnt}})/\tau_{\text{Wnt}}}+1}$
$C_{DKK1} = \frac{\beta_{DKK1}.C_{OBa}}{\widetilde{D_{DKK1}}}$	$C_{\text{DKK1}} = \frac{\beta_{\text{DKK1},T}C_T}{\widetilde{D_{\text{DKK1}}}}$
$\beta_{RANKL} = \beta_{OBp,RANKL}$	$\beta_{\text{RANKL}} = \beta_{\text{OBp,RANKL}} + \beta_{\text{T,RANKL}}$
	$C_{\text{RANKLmax}} = (R_{\text{RL,OBp}}C_{\text{OBp}} + R_{RL,T}C_T)\pi_{\text{RANKL}}^{\text{Ligand}}$
$C_{PTH} = \frac{\beta_{PTH}}{\widetilde{D_{PTH}}}$	$C_{\text{PTH}} = \frac{\beta_{\text{PTH}}+\beta_{\text{PTHrP}}C_T\pi_{\text{act,TGF}}^{\text{PTHrP}}}{\widetilde{D_{\text{PTH}}}}$
$C_{IL6} = \frac{(\beta_{IL6}C_{\text{OBa}})\pi_{\text{act,TGF}}^{\text{IL6}}}{\frac{(\beta_{\text{IL6}}C_{\text{OBa}})\pi_{\text{act,TGF}}^{\text{IL6}}}{C_{\text{IL6max}}}+\widetilde{D_{\text{IL6}}}}$	$C_{\text{IL6}} = \frac{(\beta_{\text{IL6,OBa}}C_{\text{OBa}}+\beta_{\text{IL6},T}C_T)\pi_{\text{act,TGF}}^{IL6}}{\frac{(\beta_{\text{IL6,OBa}}C_{\text{OBa}}+\beta_{\text{IL6},T}C_T)\pi_{\text{act,TGF}}^{\text{IL6}}}{C_{\text{IL6max}}}+\widetilde{D_{\text{IL6}}}}$
C_E = constant	$C_E = 8.151\times10^{1}pM$ (postmenopausal women)

3.3 Experimental study

3.3.1 ELISA assay

The ELISA assay has been used to quantify experimentally the concentration of some factors released by human active osteoblasts (HOB) and ER + breast cancer cells MCF-7. MCF-7 cells have been chosen being a BC cell line with ER + and being widely used in in vitro experimentation. HOB C-12760 and their basal growth medium have been purchased from PromoCell company; and MCF-7 ATCC® HTB-22™ with their culture medium Eagle's Minimum Essential Medium have been purchased from the American Type Culture Collection (ATCC) center.

DKK-1, IL-6, RANK, and RANKL expression have been quantified for OBa and MCF-7 cells (Table 4). In order to mimic the metastatic environment, different experimental conditions have been established (Table 5). RANK

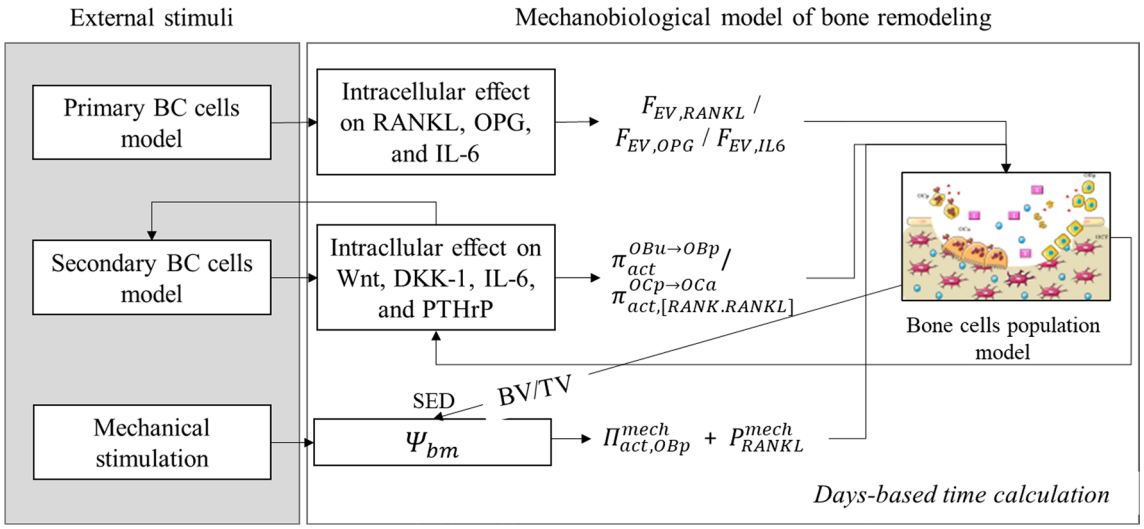

Fig. 5 Schematic representation of the algorithm of implemented model. The two-way model: (i) mechanical solicitation by the SED and (ii) biological solicitation by BC cancer effects. The primary BC drives the BR model through $F_{EV,RANKL}$, $F_{EV,OPG}$, and $F_{EV,IL6}$, while the biological feedback between BR model and metastatic BC model is mediated by Wnt, DKK-1, IL-6, and PTHrP concentrations. BV/TV values obtained from the BR update the SED value in each step

Table 4 Model parameters quantification: conditions and ELISA method description

Parameter	Definition	ELISA condition
$\beta_{OBa,DKK1}$	Production rate of DKK-1 by one OBa	ELISA condition 1 with OBa secretion
$\beta_{OBa,IL6}$	IL-6 production by one OBa per day	ELISA condition 1 with OBa secretion
$\beta_{OBp,RANKL}$	Production rate of RANKL by OBp after metastasis	ELISA condition 2 with OBa secretion
$\beta_{T,RANKL}$	Production rate of RANKL by BC tumor cells after metastasis	ELISA condition 3 with MCF-7 secretion
$\beta_{T,DKK1}$	Production rate of DKK-1 by BC tumor cells after metastasis	ELISA condition 3 with MCF-7 secretion
$\beta_{OBa,IL6}$	Production rate of IL-6 by OBa after metastasis	ELISA condition 2 with OBa secretion
$\beta_{T,IL6}$	Production rate of IL-6 by BC tumor cells after metastasis	ELISA condition 2 with MCF-7 secretion
$R_{RL,T}$	RANKL concentration expressed by one BC tumor cell surface	ELISA condition 2 with MCF-7 secretion
$\rho_{T,RANK}$	RANK concentration expressed by one BC tumor cell surface	ELISA condition 3 with MCF-7 Lyse
$\widetilde{D_{DKK1}}$	Degradation rate of DKK-1	ELISA condition 1 with MCF-7 secretion

Table 5 Cells culture conditions for ELISA assays

Cell	ELISA condition 1	ELISA condition 2	ELISA condition 3
OBa	Osteoblast growth medium	MCF-7 supernatant	–
THP-1	DMEM	MCF-7 supernatant	–
MCF-7	DMEM	OBa supernatant	THP-1 supernatant

and RANKL expression by MCF-7 has been absent in the presence of OBa supernatant. Hence, we cultured MCF-7 in THP-1 cells' supernatant, as they also exist in the bone microenvironment.

Cell-conditioned media were collected for the studied cell types, and their numbers were quantified after 24 h of secretion (Fig. 6). Using a 96-well plate we have established the ELISA protocol and determined the production rates of factors contained in a sample of cells secretion (Table 4). In contrary for $\rho_{T,\mathrm{RANK}}$ determination, MCF-7 cells' lyse containing MCF-7 fragment instead of their secretion has been used to quantify RANK number expressed on the MCF-7 cells' surfaces.

3.3.2 MTT assay

In order to determine BC tumor cells proliferation rate in primary stage (Eq. 6) (Table 6), we used the colorimetric assay named MTT. This method required an incubation for 24 h of MCF-7 cells in their culture medium DMEM by putting 100 µl/well in 96-well plate. After 24 h, the medium is aspirated and 100 µl/well of 10% MTT reagent is added to be incubated for 1 to 4 h until the cells turn purple. After 1 h, 10% MTT is aspirated and 100 µl/well of DMSO is added. Finally, the absorbance is recorded at 550 nm. According to the intensity variation, we determine the rate of MCF-7 proliferation.

3.3.3 Results of the experimental study

The results of the ELISA and MTT experiments, to determine the parameters in relation to the BC, are grouped in the table below:

3.4 Model parameters

The parameters used in our model are provided in Tables 7 and 8. Most of the parameters have been used in previous works treating BR mathematical modeling or in works studying experimentally cells behavior and their secreted biochemical factors.

4 Results and discussion

This study targets the prediction of BV/TV behavior under BC disease affecting BR process. The model predicts changes in preosteoclasts, osteoblast, and osteoclast concentrations together with changes in BV/TV.

4.1 Breast cancer effect on bone remodeling

Figure 7 represents BV/TV variation all over the different imposed conditions. In the first year, the model represented normal conditions by unchanged bone volume. Afterward, the menopause effect has been introduced leading to 0.72% of bone loss due to estrogen deficiency after 3 years. This moderate decrease in BV/TV has been observed in many experimental studies investigating age effect or menopause effect on bone quality (Table 9). At the fourth year, primary BC has been added and an anabolic action on BR has been observed leading to a 6.22% increase in BV/TV within nearly 1 year even with the persistent menopause effect. This increase was in concordance with (Chiou et al. 2021) results, that prove experimentally an increase of 2.25 and 4.25% in trabecular and cortical bone, respectively (Table 9). Finally, by secondary BC launching, a

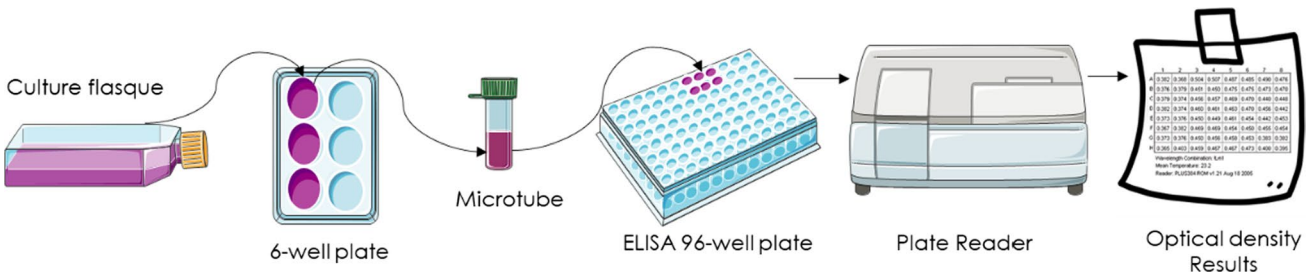

Fig. 6 General protocol of ELISA assay starting by culturing cells, extracting their supernatant, using the 96-well plate for coating, sampling, and adding factors antibodies, then extracting the results using the plate reader

Table 6 MCF-7 proliferation quantification: condition and MTT method description

Parameter	Definition	MTT condition	Description of experimentation
$P_{T'}$	Breast cancer primary tumor cell proliferation rate	MCF-7 normal medium (DMEM)	The viability of cells has been noted every 24 h for 3 days

Table 7 Parameters in the normal bone remodeling model (Bourhis et al. 2010; Wang et al. 2011; Pivonka et al. 2013; Farhat et al. 2017; Pastrama et al. 2018; Reeh et al. 2019)

Parameter	Value	Parameter	Value	Parameter	Value
C_{OBu}	3.27×10^{-6} pM	$\widetilde{D_{IL6}}$	4.99×10^{1} 1/day	$K_{rep,IL6}$	2.525×10^{4} pM
$C_{\mathrm{OBp,ini}}$	7.67×10^{-4} pM	β_{Wnt}	9×10^{-3} pM/day	$K_{act,E}$	9.2307×10^{2} pM
$C_{\mathrm{OBa,ini}}$	6.39×10^{-4} pM	β_{PTH}	9.74×10^{2} pM/day	$K_{rep,E}$	2.1×10^{2} pM
C_{OCp}	1.28×10^{-3} pM	$\beta_{\mathrm{OBp,RANKL}}$	1.62×10^{2} pM/day	$K^{OCp\rightarrow OCa}_{act,[RANK.RANKL]}$	4.79×10^{1} pM
$C_{\mathrm{OCa,ini}}$	1.07×10^{-4} pM	$\beta_{\mathrm{OBa,OPG}}$	1.63×10^{8} 1/day	$K_{A2,RANK}$	7.19×10^{-2} 1/pM
D_{OBu}	2.646×10^{2} 1/day	$K^{OBu\rightarrow OBp}_{\mathrm{act,TGF}\beta}$	4.28×10^{-4} pM	$K_{A1,OPG}$	5.68×10^{-2} 1/pM
D_{OBp}	4.65×10^{-1} 1/day	$K^{OBp\rightarrow OBa}_{\mathrm{rep,TGF}beta}$	2.49×10^{-4} pM	C_{OPGmax}	7.98×10^{2} pM
D_{OCp}	4.097 1/day	$K^{OCa\rightarrow +}_{\mathrm{act,TGF}\beta}$	4.28×10^{-4}	C_{IL6max}	8.01×10^{-1} pM
$\mathcal{P}_{\mathrm{OBp}}$	5.01×10^{2} 1/day	$K^{IL6}_{\mathrm{act,TGF}\beta}$	4.28×10^{-4} pM	$R_{RL,OBp}$	3×10^{6}
A_{OBa}	3.91×10^{-1} 1/day	$K_{\mathrm{act,PTH}}$	2.09×10^{2} pM	$\rho_{OCp,RANK}$	10000
A_{OCa}	1.2 1/day	$K_{\mathrm{rep,PTH}}$	2.21×10^{-1} pM	$\frac{\alpha k_{res} C_{OCa}}{D_{TGF\beta}}$	1
$\widetilde{D_{\mathrm{RANKL}}}$	4.16 1/day	$K_{\mathrm{act,DKK1}}$	2.09×10^{4} pM	C_E	9.175×10^{1} pM
$\widetilde{D_{\mathrm{PTH}}}$	3.84×10^{2} 1/day	$K_{\mathrm{rep,DKK1}}$	4.28×10^{-4} pM	k_{form}	3.34×10^{1}%/pM.day
$\widetilde{D_{\mathrm{OPG}}}$	4.16 1/day	$K_{\mathrm{act,Wnt}}$	1.74×10^{5} pM	k_{res}	2×10^{2}%/pM.day
$\widetilde{D_{\mathrm{Wnt}}}$	2 1/day	$K_{\mathrm{act,IL6}}$	2.525×10^{4} pM	λ	0.1
c_{bm}	$\begin{pmatrix} 18.5 & 10.3 & 10.4 & 0 & 0 & 0 \\ 10.3 & 20.8 & 11.0 & 0 & 0 & 0 \\ 10.4 & 11.0 & 28.4 & 0 & 0 & 0 \\ 0 & 0 & 0 & 12.9 & 0 & 0 \\ 0 & 0 & 0 & 0 & 11.5 & 0 \\ 0 & 0 & 0 & 0 & 0 & 9.3 \end{pmatrix}$	Σ	-30 MPa	α	1×10^{5} pM/day

Table 8 Additional parameters for bone remodeling affected by primary and secondary breast cancer (Kim et al. 2013; Kim et al. 2015; Shizu et al. 2017; Smy and Straseski, 2018; Loftus et al. 2019; Wei and Wei, 2019)

Primary breast cancer		BC metastasis	
Parameter	Value	Parameter	Value
$C_{T',ini}$	2.96×10^{-3} pM	$C_{T,ini}$	1.82×10^{-3} pM
$C_{T'max}$	3.73×10^{-2} pM	C_{Tmax}	1.82×10^{-2} pM
C_E	8.151×10^{1} pM	P_T	0.3 1/pM
$L_{EV,RANKL}$	3.43×10^{-4} 1/pM	C_E	8.151×10^{1} pM
$L_{EV,OPG}$	9.40×10^{-11} 1/pM	$\beta^{max}_{Wnt,T}$	5×10^{3} 1/day
$L_{EV,IL6}$	4.89×10^{-5} 1/pM	$\beta^{min}_{Wnt,T}$	5×10^{3} 1/day
t_{Wnt}	115 days	τ_{Wnt}	50 days

steeper decrease in BV/VT has been observed compared to menopause effect leading to a decrease of 14.14% BV/TV value in the presence of primary cells effect, and of 15.74% in the absence if primary cells effect. We remark a higher bone loss in the study of (Verbruggen et al. 2022) compared to our results (Table 9). (Verbruggen et al. 2022) noticed a 2% decrease in BV/TV only in 6 weeks using 4T1 BC cells. The nature of BC cells in addition to the probability of inducing nonlinear bone loss could be the source of the difference observed.

Keeping the same constant concentration of PTH and Wnt, we notice that during menopause estrogen concentration decrease induces a slight increase in DKK-1 and the inflammatory cytokine IL-6. Those behaviors were simultaneous to the slight but noticeable increase in OCa and OBp concentration. After (Meno/Prim) transition, we observe a moderate and a significant decrease in DKK-1 and IL-6, respectively, leading to the big decrease in OCa concentration and a moderate decrease in OBp and OBa concentrations (Fig. 8A, a).

Finally, in the (Prim/Sec) transition, we notice an increase in all the studied biochemical factors notably WNT, DKK-1, and IL-6. Concurrently to those changes, osteoclasts' concentration experienced a huge increase (Fig. 8B,b).

By increased C_{RANKLmax} due to EV particles effect in primary BC, RANKL degradation becomes highly superior to its production, leading to less RANKL concentration. Reduced RANKL suppresses osteoclastogenesis and less bone resorption reduces TGF_{β} conducts to higher differentiation of OBp (Fig. 8a).

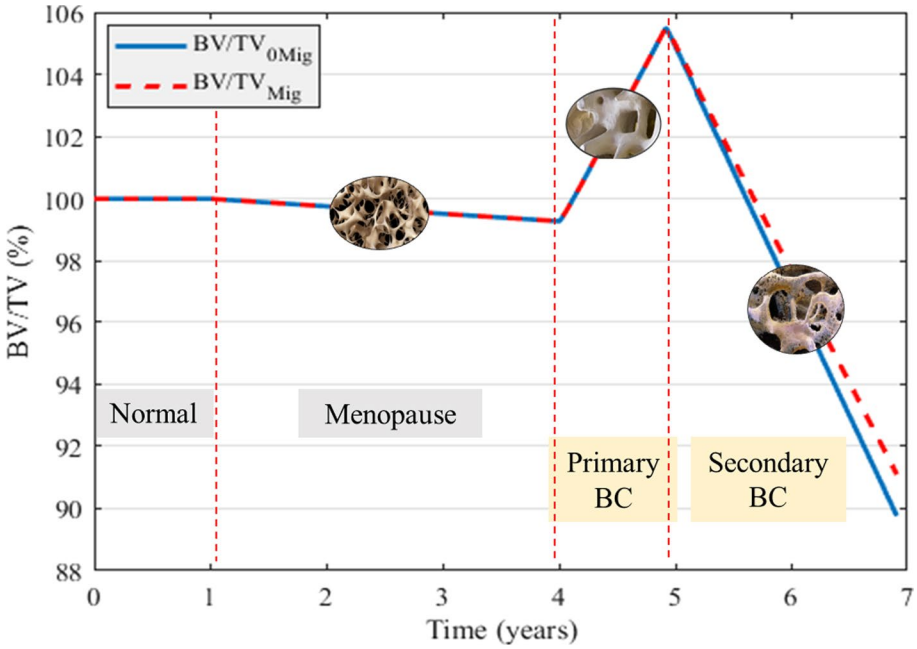

Fig. 7 Bone volume fraction change over time through four steps: (i) $0 < t < 1$ BR in normal conditions, (ii) $1 < t < 4$ BR affected by menopause, (iii) $4 < t < 4.9$ BR affected by primary breast cancer through EV's, and (iv) $4.9 < tt < 6.9$ BR affected by the direct effect of secondary breast cancer. BV/TV is considered for primary BC (i) Mig: migration during metastasis and (ii) Mig0: without migration during metastasis

Table 9 Model validation based on experimental studies. BV/TV values in experimental results have been adjusted to conform the state time considered in our numerical model

	State	Model result	Study result	Study method	Reference
BV/TV	Menopause	−0.75%	−0.98%	Women distal tibia images	(Wehrli et al. 2008)
			−0.51%	Women distal radius images	(Amin and Khosla, 2012)
	Primary BC	6.22%	2.25–4.25%	Mice proximal tibia images	(Chiou et al. 2021)
	Secondary BC	−15.74%	−32%	Mice contra lateral side of femur images	(Verbruggen et al. 2022)
			−12.17%	Bone cylindrical specimens of patients with metastatic cancer images	(Nazarian et al. 2008)
RANKL/OPG	Menopause	0.04	0.045	Measurement by the immunoradiometric method	(Liu et al. 2005)
			0.079	ELISA assay on blood samples	(Azizieh et al. 2019)
	Primary BC	0.014	0.08	ELISA assay on human blood samples	(Elfar et al. 2017)
			0.0015–2.042	ELISA assay on	(Kiechl et al. 2017)
	Secondary BC	10	0.36	ELISA assay on human blood samples	(Elfar et al. 2017)

Over the metastatic period, the inflammatory cytokine IL-6 and Wnt have extremely increased (Fig. 8B). In spite of the noticeable increase in DKK-1, Wnt kept its progressive increase by means of cancer cells effect, which enhanced OBp formation that directly stimulate osteoclastogenesis by producing more RANKL (Table 10). On the other hand, the increase in IL-6 contributed to RANKL stimulation and OPG repression. Those results explain researchers' observation of RANKL/OPG ratio increase in women with the risk of BC or which already suffer from BC (Elfar et al. 2017). According to (Rucci et al. 2004), MCF-7 ER + cells have a great potential to induce osteolytic bone lesions and stimulate osteoclastogenesis and osteoclast activity. By comparing MCF-7 to a more invasive BC cells, it has been observed that they were more aggressive vis a vis the bone microenvironment in the metastatic state provoking a noticeable bone loss. Our findings were in concordance with the experimental observations proving that breast cancer emergence induces osteolytic lesions (Gregory et al. 2013).

4.2 RANKL/OPG ratio variation in normal and affected BR:

The analysis of the biochemical factors effect on the different BR cases deems important for the comprehension of each cell behavior and bone volume fraction values as well. In this subsection, we are going to compare RANKL/OPG ratio variation in the normal BR and BR affected by primary and secondary BC. This ratio variation effect

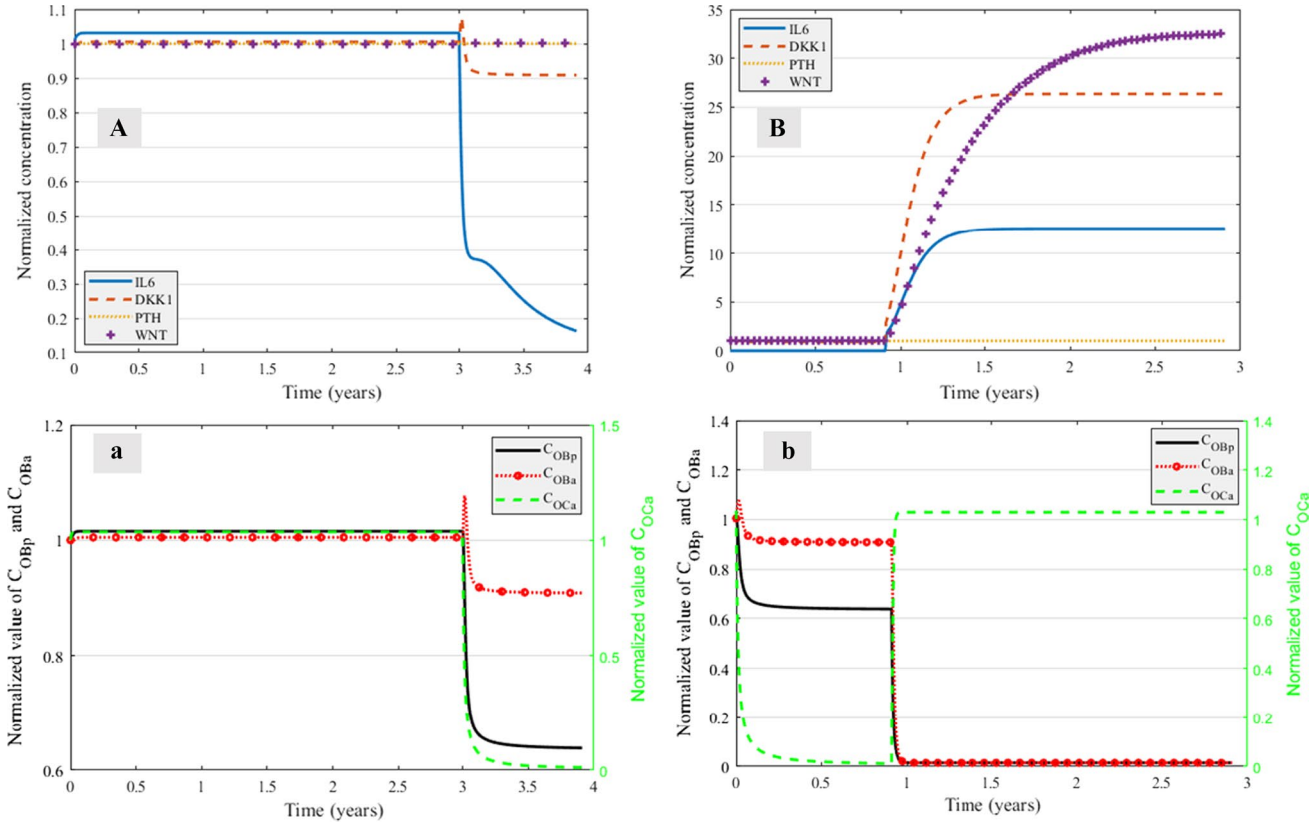

Fig. 8 Biochemical factors variation in font of bone cells concentration variation in the main two transition phases of the model. (A,a) Transition from menopause to primary BC-affected BR (Meno/Prim), and (B,b) transition from primary BC to secondary BC-affected BR (Prim/Sec). All the concentrations have been normalized based on the initial values in normal condition BR

Table 10 Results of estrogen, IL-6, and PTH domination on RANKL and OPG concentration and Wnt and TGF_β domination on OBu differentiation

Factors	Function	BR	Menopause	BR-primary BC	BR-secondary BC
Estrogen	Activation of OPG production	9.473×10^{-1}	9.473×10^{-1}	1.5092	2.096×10^{-1}
	Repression of RANKL production	2.8184	2.8185	2.9509	2.9509
IL-6	Repression of OPG production	1.9004	1.9004	3.2419×10^{-15}	3.2227×10^{-7}
	Activation of RANKL production	3.0003×10^{-5}	3.0003×10^{-5}	7.1393×10^{-16}	3.2227×10^{-7}
PTH	Repression of OPG production	1.523×10^{-1}	1.523×10^{-1}	1.4908	2.07×10^{-1}
	Activation of RANKL production	1.814×10^{-1}	1.815×10^{-1}	4.91×10^{-2}	4.91×10^{-2}
Wnt	Activation of OBu differentiation	2.5861×10^{-7}	2.5861×10^{-7}	2.5149×10^{-7}	1.08×10^{-2}
TGF_β	Activation of OBu differentiation	2	2	2	1.9892

on BV/TV is exhibited in Fig. 9. After menopause, we notice an increase in RANKL/OPG ratio simultaneously to an intense bone loss. Concerning the primary BC case, RANKL/OPG reaches low levels lifting up to nearly 0 at the beginning of BC appearance, which means that RANKL levels have been extremely decreased. Thereafter, RANKL/OPG ratio dropped comparably to the menopause case. In spite of the continuous increase in RANKL/OPG over time, its value stayed under 0.014. By the start of secondary BC, RANKL/OPG ratio has experienced an increase, which has accelerated after 1 year of BC metastasis. In contrary to primary BC, RANKL/OPG ratio levels in the metastatic BC case have been very high, which explains the excessive bone loss in this period.

RANKL/OPG ratio results were similar to the quantitative experimental studies stated in Table 9, except for the

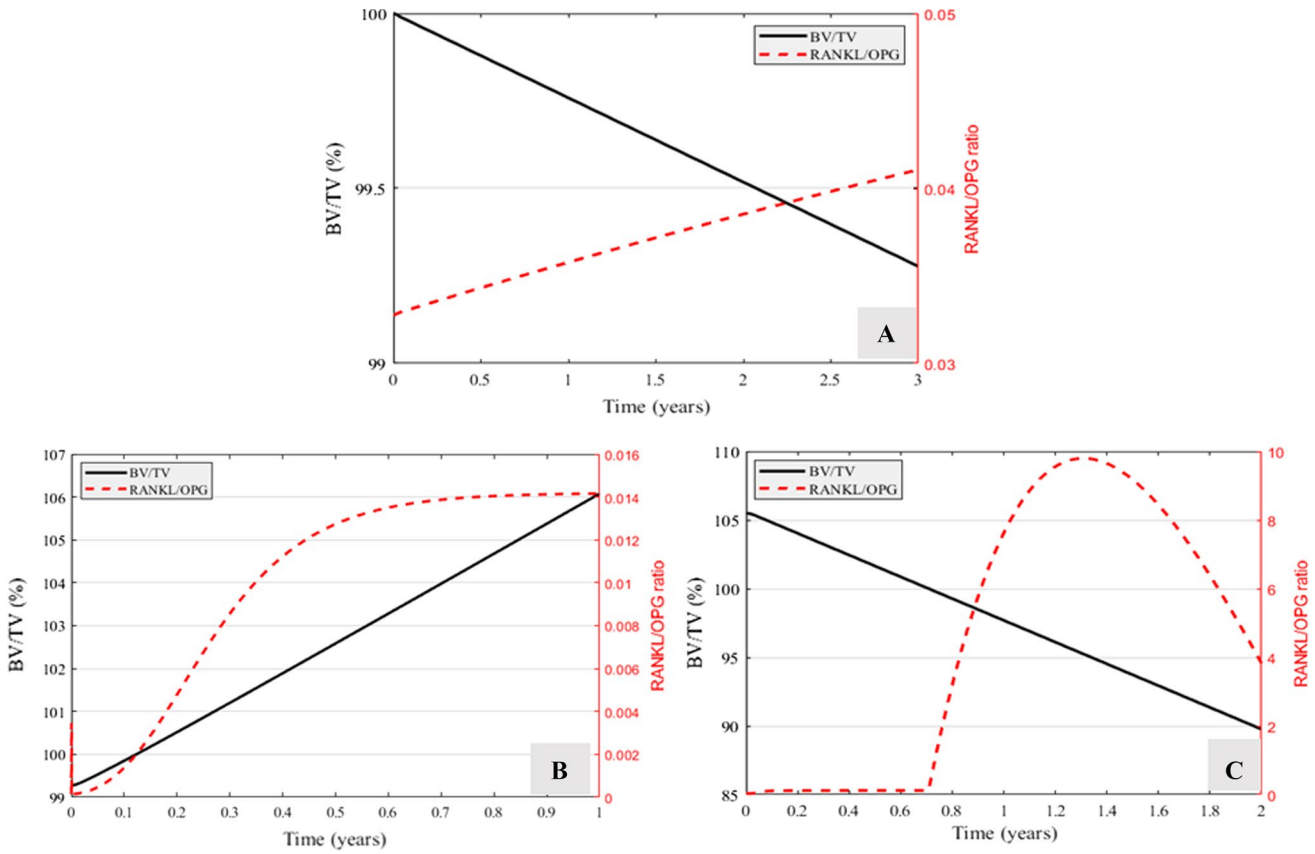

Fig. 9 RANKL/OPG ratio variation during BV/TV variation in (**a**) menopause condition, (**b**) primary BC conditions, and (**c**) secondary BC conditions

metastatic BC case where our model reveals high levels of RANKL/OPG comparably to (Elfar et al. 2017). This could be due to the difference between blood and bone microenvironment in terms of RANKL and OPG concentrations or to our over stimulation of RANKL production compared to OPG, which lead to surpass the normal levels of RANKL in the area.

4.3 Biochemical factors contribution in RANKL and OPG production

Based on the outcomes presented in Fig. 9, RANKL and OPG concentrations are the most influencing variables on BV/TV in the entire studied cases. For this reason, we studied the domination of the other biochemical factors, notably Estrogen, IL-6, and PTH, on those two concentrations' level (Table 10). Other than RANKL and OPG concentrations, we studied the domination of Wnt and TGF_{β} on osteoblasts differentiation as osteoblasts are the main RANKL and OPG secreting cells as well.

At the steady state, $\pi^{\text{Fact1}}_{\text{act/rep}}/((\pi^{\text{Fact1}}_{\text{act/rep}} + \pi^{\text{Fact2}}_{\text{act/rep}} + \pi^{\text{Fact3}}_{\text{act/rep}})/3)$ is calculated for each factor. Results have shown that in the normal case, IL-6 was dominating the control of OPG release, while RANKL concentration was mainly controlled by estrogen effect. Concerning the primary breast cancer case, OPG concentration was dominantly controlled by PTH, while RANKL concentration was mainly regulated by estrogen given the reduced IL-6 concentration (Fig. 8A). As well as primary BC case, in metastatic BC case, OPG concentration was dominated by PTH, and RANKL concentration was dominated by estrogen.

4.4 Model parameters impact

In other to quantify the effect of the biological factors' parameters in each BR–BC model, we have variated all the parameter permitting the transition from normal BR to BC-affected BR. For primary BC, first we variated each of$L_{EV,IL6}$, $L_{\text{EV,OPG}}$, and $L_{\text{EV,RANKL}}$ separately but no changes have been noticed except for $L_{EV,RANKL}$ that induced a 0.1% decrease in BV/TV. Then, we set their values at 0 and investigated the effect of each parameter on the model after being added (Fig. 10). The most influencing factor was $L_{\text{EV,RANKL}}$ leading to a very noticeable increase in BV/TV reaching

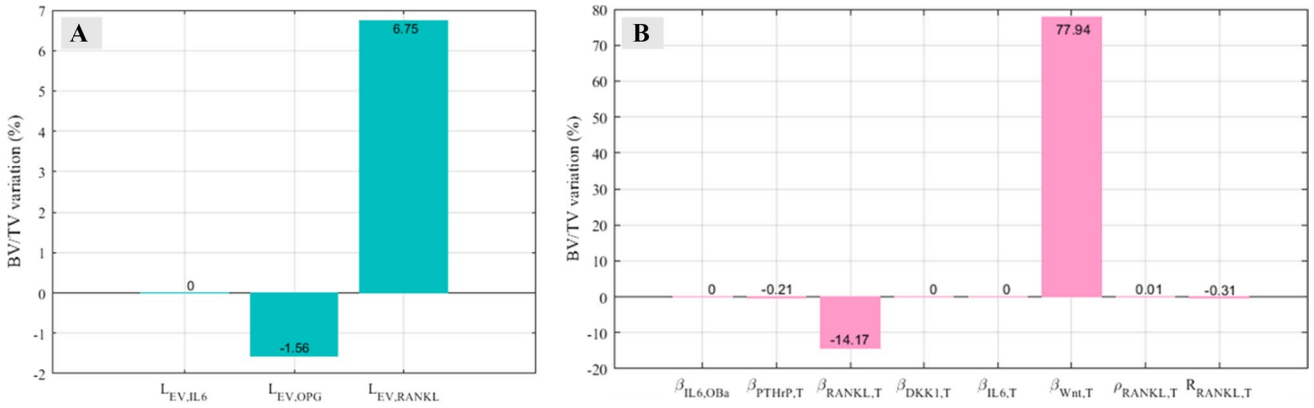

Fig. 10 BV/TV sensitivity: **a** to parameters added in BR affected by primary BC after being included separately and **b** to parameters added in BR affected by secondary BC

6.75%, then followed by $L_{\mathrm{EV,OPG}}$ that induced a 1.56% decrease in BV/TV, while $L_{\mathrm{EV,IL6}}$ had no significant effect.

For secondary BC case, we studied the effect of biochemical factors production rates effect on BV/TV behavior. In Fig. 10B, we can observe that $\beta_{T,\mathrm{Wnt}}$ was the only parameter boosting bone gain by inducing a 77.94% of BV/TV increase. Otherwise, the other parameters, except $\beta_{\mathrm{OBa,IL6}}$, $\beta_{T,\mathrm{DKK1}}$, and $\beta_{T,\mathrm{IL6}}$ led to moderate to small changes in BV/TV,$\beta_{T,\mathrm{RANKL}}$; $\beta_{T,\mathrm{PTH}rP}$, and $R_{T,\mathrm{RANKL}}$ leading, respectively, to 14.17, 0.21 and 0.31% of bone loss, and $\rho_{T,RANK}$ leading to a 0.01% of bone gain. In contrary to those parameters, the model has been very sensitive to $\beta_{\mathrm{OBp,RANKL}}$ thus, by making a small variation in this last BV/TV has dropped by 36.78%. Under all those results, we conclude that RANKL production alteration is the most critical parameter in both models. Those results show that breast cancer still has more influence on bone remodeling regardless of the available estrogen concentration. Not to mention that estrogen enhances tumor cells growth, thereby enhancing cancer's negative impact on the bone.

5 Conclusion

In this work, we propose a BR–BC mathematical model where parameters are experimentally determined. The obtained results were in agreement with initial assumptions of the model, with literature, and with experimental studies results whether in terms of BV/TV or RANKL/OPG ratio. In the model, (i) RANKL production was the main controlling parameter of the primary BC–BR model being able to reflect the osteoblastic lesions caused by EV's action, (ii) The vicious cycle represented in the secondary BC–BR model has been able to reflect the osteolytic lesions caused by BC metastasis, and (iii) BC had higher effect on BR than menopause.

The experimentations elaborated in this work permitted us to reflect the real response and influence of each biochemical factor involved in the remodeling and to make some assumption regarding the primary BC distant effect phenomenon, which is not quite investigated by biologists. However, taking into consideration many parameters made the models complicated and hard. In addition, a perfect in vitro representation of the metastatic environment has been difficult to create, which could influence our results to some extent. Besides, considering instantaneous mineralization could limit the accuracy of the results especially while integrating primary BC that affects mineralization. For these reasons, we aim in our future works to reduce the model parameters, find a method permitting to create a more realistic experimentation conditions, and to consider the mineralization effect in the model.

Appendix

Bone remodeling general model

The general mathematical model formulation of bone cell behavior is presented as follows, where the bone cells involved are: Osteoblast precursors (OBp), active osteoblast (OBa), and active osteoclasts (OCa) (Pivonka et al. 2008):

Table 11 Description of the biochemical and mechanical factors' integration into the normal BR model

Factor	Function	Factor concentration
TGFβ	$\pi_{\text{act}}^{\text{OBu}\rightarrow\text{OBp}} = \left(\pi_{\text{act,TGF}\beta}^{\text{OBu}\rightarrow\text{OBp}} + \pi_{\text{act,Wnt}}^{\text{OBu}\rightarrow\text{OBp}}\right) + (\pi_{\text{act,TGF}\beta}^{\text{OBu}\rightarrow\text{OBp}}\pi_{\text{act,Wnt}}^{\text{OBu}\rightarrow\text{OBp}})$	$C_{\text{TGF}\beta} = \frac{\alpha k_{\text{res}} C_{OCa} + S_{\text{TGF}\beta}}{\widetilde{D_{\text{TGF}\beta}}}$
Wnt		$C_{\text{Wnt}} = \frac{\beta_{\text{Wnt}}\pi_{\text{rep,DKK1}}}{\widetilde{D_{\text{Wnt}}}}$
DKK-1		$C_{\text{DKK1}} = \frac{\beta_{\text{DKK1}} C_{\text{OBa}}}{\widetilde{D_{\text{DKK1}}}}$
RANK/RANKL/OPG	$\pi_{\text{act,[RANK.RANKL]}}^{\text{OCp}\rightarrow\text{OCa}} = \frac{C_{\text{OCp,[RANK.RANKL]}}}{K_{\text{act,[RANK.RANKL]}}^{\text{OCp}\rightarrow\text{OCa}} + C_{\text{OCp,[RANK.RANKL]}}}$	$C_{\text{OCp,[RANK.RANKL]}} = K_{a,\text{[RANK.RANKL]}} C_{\text{RANKL}} C_{\text{OCp,RANK}}$
		$C_{\text{OCp,RANK}} = \rho_{\text{OCp,RANK}} C_{OCp}$
		$C_{\text{RANKL}} = \frac{C_{\text{RANKLmax}}}{(1+K_{\text{A1,OPG}} C_{\text{OPG}} + K_{\text{A2,RANK}} C_{\text{OCp,RANK}})} (\frac{\beta_{\text{OBp,RANKL}} + P_{\text{RANKL}}^{\text{mech}}}{\beta_{\text{OBp,RANKL}} + \widetilde{D_{\text{RANKL}}} C_{\text{RANKLmax}}})$
		$C_{\text{RANKLmax}} = R_{\text{RL,OBp}} C_{\text{OBp}} \pi_{\text{RANKL}}^{\text{Ligand}}$
		$C_{\text{OPG}} = \frac{(\beta_{OBa,\text{OPG}} C_{OBa}) \pi_{OPG}^{Ligand}}{\frac{(\beta_{OBa,\text{OPG}} C_{OBa}) \pi_{rep,OPG}^{Ligand}}{C_{OPGmax}} + \widetilde{D_{OPG}}}$
		$P_{\text{RANKL}}^{mech} = \begin{cases} \alpha\left(1 - \frac{\Psi_{bm}}{\Psi_{bm}(t_0)}\right), & \Psi_{bm} < \Psi_{bm}(t_0) \\ 0 & \Psi_{bm} \geq \Psi_{bm}(t_0) \end{cases}$
PTH, IL-6	$\pi_{RANKL}^{Ligand} = \left(\pi_{act,RANKL}^{PTH} + \pi_{act,RANKL}^{IL6} + \pi_{rep,RANKL}^{E}\right) + \left(\pi_{act,RANKL}^{PTH}\pi_{rep,RANKL}^{E}\right) - (\pi_{act,RANKL}^{PTH}\pi_{act,RANKL}^{IL6}$	$C_{PTH} = \frac{\beta_{PTH}}{\widetilde{D_{\text{PTH}}}}$
	$\pi_{OPG}^{Ligand} = \left(\pi_{rep,OPG}^{PTH} + \pi_{rep,OPG}^{IL6} + \pi_{act,OPG}^{E}\right) + \left(\pi_{rep,OPG}^{PTH}\pi_{act,OPG}^{E}\right) - (\pi_{rep,OPG}^{PTH}\pi_{rep,OPG}^{IL6})$	$C_{IL6} = \frac{(\beta_{IL6} C_{OBu}) \pi_{act,TGF}^{IL6}}{\frac{(\beta_{IL6} C_{OBu}) \pi_{act,TGF}^{IL6}}{C_{IL6max}} + \widetilde{D_{IL6}}}$
		$C_E = 9.175 \times 10^2 pM$ (*healthywomen*)
Mechanical	$\Pi_{\text{act,OBp}}^{\text{mech}} = \begin{cases} \frac{1}{2} & \Psi_{bm} \leq \Psi_{bm}(t_0) \\ \frac{1}{2}\left(1 + \lambda\left(\frac{\Psi_{bm}}{\Psi_{bm,\text{min}}} - 1\right)\right) & \Psi_{bm}(t_0) < \Psi_{bm} \leq {\Psi_{bm}}^* \\ 1 & {\Psi_{bm}}^* \leq \Psi_{bm} \end{cases}$	$\Psi_{bm} = \Psi_{bm}(\Sigma, c_{bm}, (1 - \text{BV/TV}))$ ${\Psi_{bm}}^* = (1 + \lambda^{-1})\Psi_{bm}(t_0)$

$$\begin{cases} \dfrac{dC_{\mathrm{OBp}}(t)}{dt} = D_{\mathrm{OBu}}\pi_{\mathrm{act}}^{\mathrm{OBu}\to\mathrm{OBp}}C_{\mathrm{OBu}} + \mathcal{P}_{\mathrm{OBp}}\Pi_{\mathrm{act,OBp}}^{\mathrm{mech}}C_{\mathrm{OBp}} - D_{\mathrm{OBp}}\pi_{\mathrm{rep,TGF}\beta}^{\mathrm{OBp}\to\mathrm{OBa}}C_{\mathrm{OBp}} \\ \dfrac{dC_{\mathrm{OBa}}(t)}{dt} = D_{\mathrm{OBp}}\pi_{\mathrm{rep,TGF}\beta}^{\mathrm{OBp}\to\mathrm{OBa}}C_{\mathrm{OBp}} - A_{\mathrm{OBa}}C_{\mathrm{OBa}} \\ \dfrac{dC_{\mathrm{OCa}}(t)}{dt} = D_{\mathrm{OCp}}\pi_{\mathrm{act,[RANK.RANKL]}}^{\mathrm{OCp}\to\mathrm{OCa}}C_{\mathrm{OCp}} - A_{\mathrm{OCa}}\pi_{\mathrm{act,TGF}\beta}^{\mathrm{OCa}\to+}C_{\mathrm{OCa}} \end{cases} \quad \text{(A1-A3)}$$

C_{OBu}, C_{OBp}, C_{OBa}, C_{OCp}, C_{OCa} represent, respectively, OBu concentration, OBp concentration, OBa concentration, OCp concentration, and OCa concentration. D_{OBu}, D_{OBp} and D_{OCp} are, respectively, differentiation rates of OBu, OBp, and OCp. $\mathcal{P}_{\mathrm{OBp}}$ is the proliferation rate of the OBp and A_{OBa} and A_{OCa} represent, respectively, the apoptosis rates of OBa and OCa.

In Eqs. 1, 2, $\pi_{\mathrm{act}}^{\mathrm{OBu}\to\mathrm{OBp}}$, $\pi_{\mathrm{rep,TGF}\beta}^{\mathrm{OBp}\to\mathrm{OBa}}$, and $\Pi_{\mathrm{act,OBp}}^{\mathrm{mech}}$ represent, respectively, the ability of TGF_{β} and Wnt to stimulate the natural differentiation of OBu into OBp, the ability of TGF_{β} to inhibit the natural differentiation of OBp into OBa, and the ability of mechanical strains to promote pre-osteoblasts' proliferation.

In Eq. 3, $\pi_{\mathrm{act,TGF}\beta}^{\mathrm{OCa}\to+}$. $\pi_{\mathrm{act,[RANK.RANKL]}}^{\mathrm{OCp}\to\mathrm{OCa}}$ and $\pi_{\mathrm{act,TGF}\beta}^{\mathrm{OCa}\to+}$ represent, respectively, the ability of RANK/RANKL binding to promote preosteoblasts' differentiation and the ability of the TGF_{β} to stimulate active osteoclasts' apoptosis.

The fraction of extravascular bone matrix BV/TV behavior is determined by Eq. 4. BV/TV depends on active osteoblasts and osteoclasts' concentrations, where k_{form} and k_{res} represent, respectively, the daily volume of bone matrix formed by osteoblast and the daily volume of bone matrix resorbed by osteoclast.

$$\frac{d\mathrm{BV/TV}(t)}{dt} = \left(k_{\mathrm{form}}C_{\mathrm{OBa}} - k_{\mathrm{res}}C_{\mathrm{OCa}}\right) \quad \text{(A4)}$$

Seeking to represent the cellular response to ligand stimulation, Hill function has been used. The Hill activation and repression functions used in the model are expressed as follows

$$\begin{aligned} \pi_{\mathrm{act}} &= \frac{C_X}{K_{\mathrm{act}} + C_X} \\ \pi_{\mathrm{rep}} &= \frac{K_{\mathrm{rep}}}{K_{\mathrm{rep}} + C_X} \end{aligned} \quad \text{(A5)}$$

where C_X is the concentration of the ligand X governing the cellular response, and K_{act} and K_{rep} are, respectively, the activation and repression constants.

The cellular response to different ligands of the model parameters are grouped in Table 11.

Acknowledgements This work was supported by the Partenariat Hubert Curien Franco-Moroccan TOUBKAL (PHC Toubkal) No. TBK/20/102—CAMPUS No. 43681QG.

Declaration

Conflict of interest The authors declare no conflict of interest associated with this article.

References

Ait Oumghar I, Barkaoui A, Chabrand P (2020) Toward a mathematical modeling of diseases' impact on bone remodeling: technical review. Front Bioeng Biotechnol, p. 1236. https://doi.org/10.3389/fbioe.2020.584198.

Amin S, Khosla S (2012) Sex- and age-related differences in bone microarchitecture in men relative to women assessed by high-resolution peripheral quantitative computed tomography. J Osteoporosis. https://doi.org/10.1155/2012/129760

Azizieh FY et al (2019) Circulatory levels of RANKL, OPG, and oxidative stress markers in postmenopausal women with normal or low bone mineral density. Biomarker Insights, 14. https://doi.org/10.1177/1177271919843825

Bhardwaj P et al (2019) Estrogens and breast cancer: mechanisms involved in obesity-related development, growth and progression. J Steroid Biochem Mol Biol. https://doi.org/10.1016/j.jsbmb.2019.03.002

Blake M et al (2014) RANK expression on breast cancer cells promotes skeletal metastasis. Clin Exp Metastasis 31(2):233–245. https://doi.org/10.1007/S10585-013-9624-3

Bourhis E et al (2010) Reconstitution of a Frizzled8·Wnt3a·LRP6 signaling complex reveals multiple Wnt and Dkk1 binding sites on LRP6. J Biol Chem 285(12):9172–9179. https://doi.org/10.1074/jbc.M109.092130

Chiou AE et al (2021) Breast cancer–secreted factors perturb murine bone growth in regions prone to metastasis. Am Assoc Advancement Sci 7(12):eabf2283. https://doi.org/10.1126/sciadv.abf2283.

Clézardin P (2011) Therapeutic targets for bone metastases in breast cancer. Breast Cancer Res, pp. 1–9. https://doi.org/10.1186/bcr2835.

De Mukhopadhyay K et al (2015) Aromatase expression increases the survival and malignancy of estrogen receptor positive breast cancer cells. PLoS ONE. https://doi.org/10.1371/journal.pone.0121136

Elfar GA et al (2017) Validity of osteoprotegerin and receptor activator of NF-κB ligand for the detection of bone metastasis in breast cancer. Oncol Res 25(4):641–650. https://doi.org/10.3727/096504016X14768398678750

Farhat A et al (2017) An integrative model of prostate cancer interaction with the bone microenvironment. Math Biosci 294:1–14. https://doi.org/10.1016/j.mbs.2017.09.005.

Frost HM (1969) Tetracycline-based histological analysis of bone remodeling. Calcif Tissue Res 3:211–237. https://doi.org/10.1007/bf02058664

Gregory LS et al (2013) Breast cancer cells induce osteolytic bone lesions in vivo through a reduction in osteoblast activity in mice. PLOS ONE 8(9):e68103. https://doi.org/10.1371/JOURNAL.PONE.0068103

Kasoha M et al (2018) Dickkopf-1 (Dkk1) protein expression in breast cancer with special reference to bone metastases. Clin Exp Metastasis 35(8):763–775. https://doi.org/10.1007/S10585-018-9937-3

Kiechl S et al (2017) Aberrant regulation of RANKL/OPG in women at high risk of developing breast cancer. Oncotarget. https://doi.org/10.18632/oncotarget.14013.

Kiesel L, Kohl A (2016) Role of the RANK/RANKL pathway in breast cancer. Maturitas. 86:10–16. https://doi.org/10.1016/j.maturitas.2016.01.001

Kim JY et al (2013) Prognostic effect of preoperative serum estradiol level in postmenopausal breast cancer. BMC Cancer 13(1):1–6. https://doi.org/10.1186/1471-2407-13-503

Kim EK et al (2015) First evidence that Ecklonia cava-derived dieckol attenuates MCF-7 human breast carcinoma cell migration. Mar Drugs 13(4):1785–1797. https://doi.org/10.3390/MD13041785

Komarova SV et al (2003) Mathematical model predicts a critical role for osteoclast autocrine regulation in the control of bone remodeling. Bone 33(2):206–215. https://doi.org/10.1016/S8756-3282(03)00157-1

Kozlow W, Guise TA (2005) Breast cancer metastasis to bone: mechanisms of osteolysis and implications for therapy. J Mammary Gland Biol Neoplasia 10(2):169–180. https://doi.org/10.1007/S10911-005-5399-8

Labrie F (2015) All sex steroids are made intracellularly in peripheral tissues by the mechanisms of intracrinology after menopause. J Steroid Biochem Mol Biol. https://doi.org/10.1016/j.jsbmb.2014.06.001

Lamb R et al (2013) Wnt pathway activity in breast cancer sub-types and stem-like cells. PLOS ONE 8(7):e67811. https://doi.org/10.1371/JOURNAL.PONE.0067811

Lemaire V et al (2004) Modeling the interactions between osteoblast and osteoclast activities in bone remodeling. J Theor Biol 229(3):293–309. https://doi.org/10.1016/j.jtbi.2004.03.023

Liu JM et al (2005) Relationships between the changes of serum levels of OPG and RANKL with age, menopause, bone biochemical markers and bone mineral density in Chinese women aged 20–75. *Calcified Tissue International* Calcif Tissue Int 76(1):1–6. https://doi.org/10.1007/S00223-004-0007-2

Loftus A et al (2019) Extracellular vesicles from osteotropic breast cancer cells affect bone resident cells. https://doi.org/10.1002/jbmr.3891.

Lumachi F (2015) Current medical treatment of estrogen receptor-positive breast cancer. World J Biol Chem. https://doi.org/10.4331/wjbc.v6.i3.231

Del Monte U (2009) Does the cell number 10(9) still really fit one gram of tumor tissue? Cell Cycle 8(3):505–506. https://doi.org/10.4161/CC.8.3.7608.

Mullender MG, Huiskes R (1997) Osteocytes and bone lining cells: Which are the best candidates for mechano-sensors in cancellous bone? Bone. https://doi.org/10.1016/S8756-3282(97)00036-7

Mundy GR (2002) Metastasis to bone: causes, consequences and therapeutic opportunities. *Nature Reviews Cancer* Nat Rev Cancer 2(8):584–593. https://doi.org/10.1038/NRC867

Nazarian A et al (2008) Bone volume fraction explains the variation in strength and stiffness of cancellous bone affected by metastatic cancer and osteoporosis. Calcif Tissue Int 83(6):368–379. https://doi.org/10.1007/S00223-008-9174-X

Oumghar IA, Barkaoui A, Chabrand P (2021) Mechanobiological behavior of a pathological bone. IntechOpen. https://doi.org/10.5772/INTECHOPEN.97029

Pastrama MI et al (2018) A mathematical multiscale model of bone remodeling, accounting for pore space-specific mechanosensation. Bone 107(May 2018):208–221. https://doi.org/10.1016/j.bone.2017.11.009.

Pivonka P et al (2008) Model structure and control of bone remodeling: a theoretical study. Bone. https://doi.org/10.1016/j.bone.2008.03.025

Pivonka P et al (2013) The influence of bone surface availability in bone remodelling—a mathematical model including coupled geometrical and biomechanical regulations of bone cells. Eng Struct 47:134–147. https://doi.org/10.1016/j.engstruct.2012.09.006

Reeh H et al (2019) 'Response to IL-6 trans- and IL-6 classic signalling is determined by the ratio of the IL-6 receptor α to gp130 expression: fusing experimental insights and dynamic modelling. BioMed Central 17(1):1–21. https://doi.org/10.1186/S12964-019-0356-0

Rucci N et al (2004) In vivo bone metastases, osteoclastogenic ability, and phenotypic characterization of human breast cancer cells. *Bone* Bone 34(4):697–709. https://doi.org/10.1016/J.BONE.2003.07.012

Salamanna F et al (2018) Link between estrogen deficiency osteoporosis and susceptibility to bone metastases: A way towards precision medicine in cancer patients. Breast. https://doi.org/10.1016/j.breast.2018.06.013

Scheiner S, Pivonka P, Hellmich C (2013) Coupling systems biology with multiscale mechanics, for computer simulations of bone remodeling. Comput Methods Appl Mech Eng 254:181–196. https://doi.org/10.1016/j.cma.2012.10.015

Shizu I et al (2017) Breast volume measurement by recycling the data obtained from 2 routine modalities, mammography and magnetic resonance imaging. ePlasty, 17.

Smy L, Straseski JA (2018) Measuring estrogens in women, men, and children: Recent advances 2012–2017. Clin Biochem 62:11–23. https://doi.org/10.1016/J.CLINBIOCHEM.2018.05.014

Verbruggen ASK et al (2022) Temporal and spatial changes in bone mineral content and mechanical properties during breast-cancer bone metastases. Bone Reports 17:101597. https://doi.org/10.1016/J.BONR.2022.101597

Wang Y et al (2011) Computational modeling of interactions between multiple myeloma and the bone microenvironment. PLoS ONE 6:e27494. https://doi.org/10.1371/journal.pone.0027494

Wehrli FW et al (2008) In vivo magnetic resonance detects rapid remodeling changes in the topology of the trabecular bone network after menopause and the protective effect of estradiol. J Bone Miner Res 23(5):730–740. https://doi.org/10.1359/JBMR.080108

Wei H-C, Wei H-C (2019) Mathematical modeling of tumor growth: the MCF-7 breast cancer cell line. Am Inst Math Sci 16(6):6512–6535. https://doi.org/10.3934/MBE.2019325